

Fabrication of an Induction Coil Magnetometer for Geomagnetic Field Measurement.

A.A. Adetoyinbo¹; O.S. Hammed^{2*} and B.O. Ogunsua¹

¹Department of Physics, University of Ibadan, Ibadan, Nigeria.

²Department of Physical Sciences, Bells University of Technology, Ota, Nigeria.

E-mail: hammedolaide@yahoo.com*

ABSTRACT

The measurement of magnetic variations within the low frequency range of 0.1 to 40Hz requires a highly sensitive magnetometer. A magnetometer based on the induction coil principle was designed, simulated, and constructed in this research. The search coil was designed by winding 4,500 turns of insulated coil on PVC pipe with 3 silicon-iron strips mounted on the PVC for higher magnetic susceptibility. The sensory method of the coil is based on the faraday's law of electromagnetic induction. The output of the coil was amplified and filtered with a band pass electronic system designed to pass the desired frequency range of 0.1 to 40Hz. A simple calibration system using the Helmholtz coil pair was designed for the calibration of the sensor to determine the conversion factor of the output root mean square (r.m.s.) voltage with the external magnetic field (Hs), since the Helmholtz coil can generate very uniform magnetic field up to 25% or more of the covered area from the centre axis. The output voltage and applied magnetic field obtained as the calibration data were fitted into a linear graph. A relatively high sensitivity of 299mv/ μ T was obtained.

(Keywords: search coil, sensor, electromagnetic induction and band pass)

INTRODUCTION

The Earth's magnetic field is a continuous varying composite field, consisting of different magnetic fields from a variety of sources which includes: the Earth's conducting fluid outer core; the Earth's crust/upper mantle; the ionosphere; the magnetosphere, and also some other sources that lead to the variations in the magnetic field. The Earth's crust consists of 90% of the geomagnetic field and it is seen as the main field. Other

magnetic fields due to the ionosphere, the magnetosphere, and the Earth's crust/upper mantle are measured as variations relative to the "Main Magnetic Field" (the field due to the Earth's conducting fluid outer core).

Magnetic field measurements are very useful for the study of the geological features that constitute the variations of the Earth's geomagnetism. The phenomena like equatorial electrojet and auroral electrojet can be observed using geomagnetic measurement techniques.

Magnetic methods are also used in oil exploration to determine depth of the basement rock and in mineral exploration to detect magnetic minerals or to locate dykes.

In archeological surveys, the knowledge of magnetic field measurement is used to detect buried artifacts, gravesites, and other cultural resources. It is also used for the location of ferrous or metallic objects like underground storage tanks, etc. The need for the measurement of magnetic fields has led to the development of different sensors and instruments. One of these instruments or sensors is known as the induction coil magnetometer.

The induction coil sensor (known as the pick-up coil sensor, search coil sensor, or the magnetic antenna) is one of the oldest and most well known magnetic sensors. It is typically an AC magnetic field measuring instrument and its advantages includes its ability to investigate AC fields within several mHz range up to MHz range, even though some special designs can measure up to GHz range [1]. Induction coil sensors are reliable, rugged, and easy to handle. The electronic system can be easily designed for the processing of the signal from the sensor with low energy consumption.

THEORY OF OPERATIONS

The design of the induction coil is based on the faraday's law of electromagnetic induction where the electromotive force (EMF) induced on the coil by the magnetic flux is given as:

$$V = -N \frac{d\Phi}{dt} \quad (1)$$

which is the same as,

$$V = -NA \frac{dB}{dt} \quad (2)$$

where Φ is $B \times A$ and $B = \mu_0 H$, then:

$$V = -\mu_0 NA \frac{dH}{dt} \quad (3)$$

In the presence of a ferromagnetic core the expression above becomes:

$$V = -\mu_0 \mu_r NA \frac{dH}{dt} \quad (4)$$

where:

- V is the EMF induced by the magnetic field
- Φ is the magnetic flux density
- B is the magnetic flux
- H is the magnetic field intensity
- N is the number of turns of the coil
- A is the area of the coil
- μ_0 and μ_r are the permeabilities of air and the ferromagnetic material, respectively.

The sensitivity of the coil depends greatly on the number of turns and the active area. The higher the value of these two parameters in a sensor designed, the higher the sensitivity. For a coil designed with the air core, the active area is usually large such that the coil may be too cumbersome to handle. For this reason, soft ferromagnetic cores are normally used to improve the sensitivity at a smaller active area. This makes the coils appear less bulky. This is due to the fact that the modern soft magnetic materials exhibit relative permeability, μ_r , even larger than 10^5 which can significantly increase the sensitivity of the sensor (Equation (4)). However, it should

be taken into account that the resultant permeability core μ_c can be much lower than the relative permeability of the core material, due to the demagnetizing field effect expressed by the geometry dependent demagnetizing factor N :

$$\mu_c = \frac{\mu_r}{1 + N \cdot (\mu_r - 1)} \quad (5)$$

Thus, the relative permeability and the resultant permeability of the core μ_c depend on the demagnetizing factor N as shown in Equation 5. This simply means that the sensitivity depends mostly on the geometry and the dimension of the coil [1].

The frequency response is such that the induction coil sensors can pass AC signals only since it cannot pass DC signals. The term DC magnetic field can be understood as a relative one. By using a sensitive amplifier and a large coil sensor, it is possible to determine the magnetic fields starting from frequency of several mHz [2, 3]. Thus, it is also possible to investigate some quasi-constant magnetic field with the stationary or unmovable coil sensor [1].

With the coil sensors, AC magnetic field with frequencies in the MHz range can be investigated. In special designs, the bandwidth can be extended to GHz range [4, 5].

METHODOLOGY

Construction of the Sensor

Three silicon iron sheets, each 0.04 inch thick, were attached and tightened on a 50cm length of 50mm diameter PVC pipe. The insulated coil of 4500 turns was wound round the PVC pipe for higher magnetic susceptibility as shown in Figure 1. The coil was sectioned into 10 layers at 450 turns per layer. This sensor was built based on the faraday's law of magnetic induction where the electromagnetic frequency induced is given by,

$$e = -N \frac{d\phi}{dt}$$

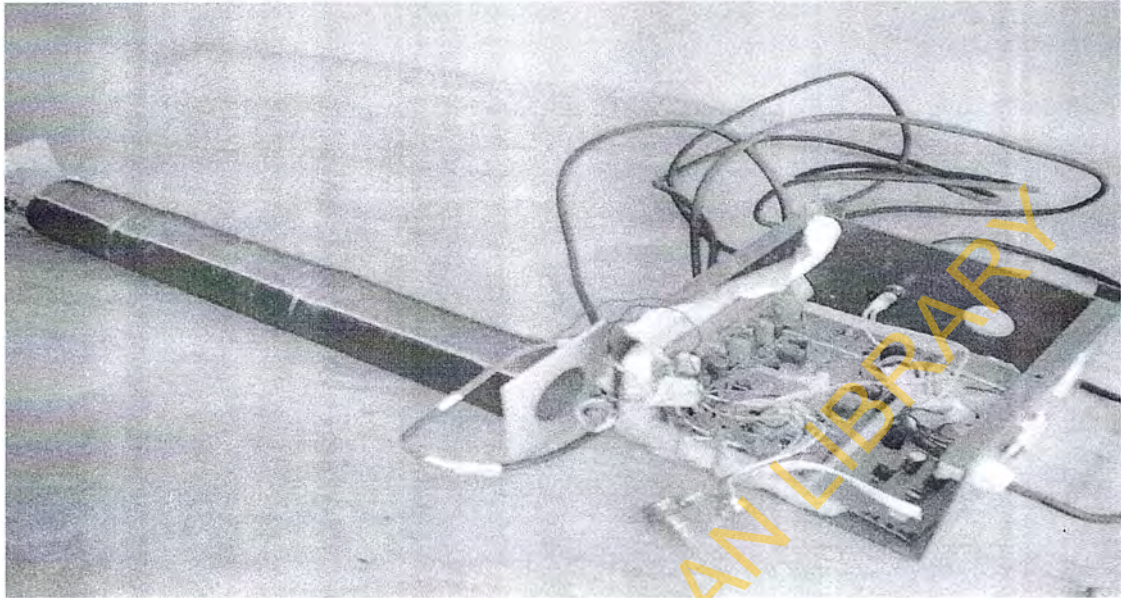


Figure 1: The Electronic System and the Sensor (Coil Wound around the PVC Pipe).

The Electronic System Design

The signal from the sensor was fed into a high gain low pass active filter which cuts off at 40Hz. Then the signal from the low pass filter was fed into a unity gain T-notch filter which filtered off the narrow band of 50Hz which might have been insinuated with desired signal through the interference from AC power lines and ripple voltages of the power supply.

The output of the notch filter was fed into a 2-pole Butterworth low pass filter to control the filtering of the higher harmonics from 50Hz upwards and also to cut off the lower end of the band below 0.1 Hz. The output signal was passed to a DC control circuit for correction of DC drifts in the signal and then fed into a 6-pole Butterworth low pass filter to further filter off excess higher harmonics at a much steeper roll off of 120 dB per decade. The final output was amplified with an output amplifier (Figure 2).

The High Gain Low-Pass Filter: This stage, as shown in Figure 3, was designed to pass frequencies below 40Hz since the cut-off frequency is given as:

$$f_p = \frac{1}{2\pi C_f R_f} = \frac{1}{2\pi \times 1 \times 10^{-6} \times 3.9 \times 10^4} = 40.8$$

$$R_f = \frac{1}{2\pi C_0 C_f} = \frac{1}{2\pi \times 40 \times 1 \times 10^{-6}} = 3.98 k\Omega$$

Since the input is non-inverting:

$$A_v = \frac{Z_f}{R_i} + 1$$

$$Z_f = \frac{X_{CF} R_f}{\sqrt{R_f^2 + X_{CF}^2}}$$

$$\text{where } X_{CF} = \frac{1}{2\pi f C_f} = \frac{1}{2\pi(40 \times 1)} \approx 3.98 k\Omega$$

$$Z_f = \frac{3.98 \times 3.98 \times 10^3}{\sqrt{(3.98 \times 10^3)^2 + (3.98 \times 10^3)^2}} = 2.814 k\Omega$$

$$A_v = \frac{Z_f}{R_i} + 1 = \frac{2814}{7.5} + 1 = 375 + 1 = 376$$

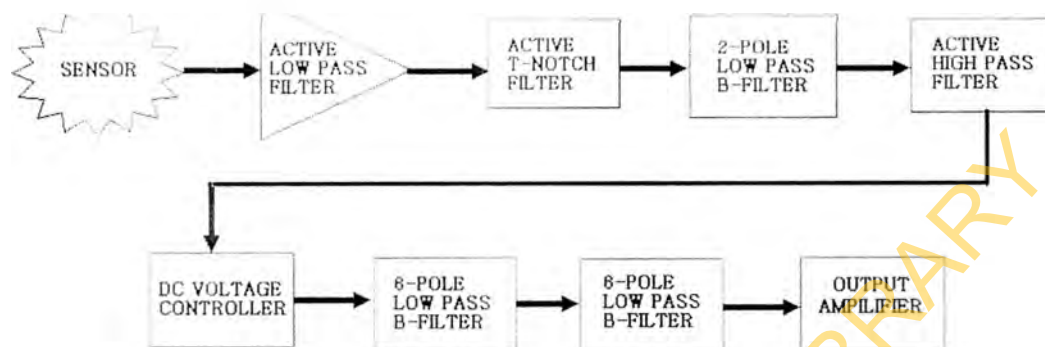


Figure 2: Block Diagram for the Electronic System.

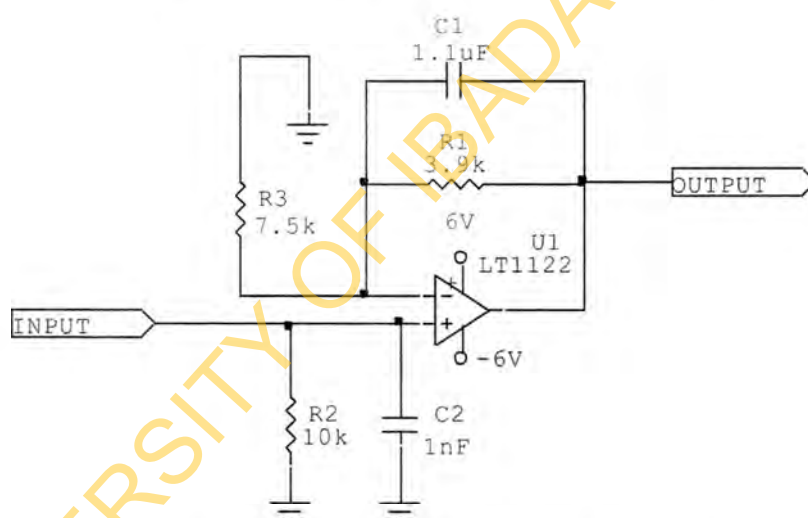


Figure 3: High Gain Input Active Low-Pass Filter

The T-Notch Filter: The notch filter shown in Figure 4 is a band reject filter designed to reject the flow of a particular frequency. Here, the frequency to be rejected is 50Hz so as to remove the interference of AC signals from the power lines. Since our designed frequency is 50Hz, the convenient standard capacitance value was chosen to calculate the value of the capacitance, C_f . And for notch filters:

$$C = C_1 = C_2 = C_3 = C_4$$

$$\text{or } C = C_1 = C_2 = \frac{C_3 + C_4}{2}$$

$$R = R_1 = R_2 = 2R_3$$

where C is chosen as 4.7 pf

$$\text{and } R = \frac{1}{2\pi \times 50 \times 4.7 \times 10^{-9}} = 677255.07702$$

$$R \approx 677.3k\Omega$$

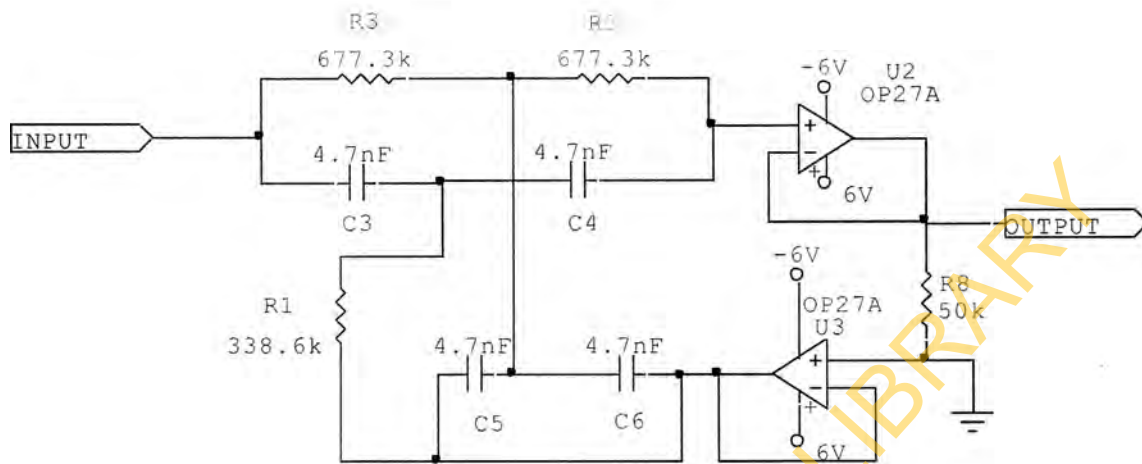


Figure 4: Unity Gain T-notch Active Filter.

This implies that $R_1=R_2=677.3$ and $R_3=338.65$. The notch filter in the circuit was designed as a unity gain filter; therefore there is no voltage gain.

$$R_{22} = R_1 (0.5858)$$

Choosing standard value of $39 \text{ k}\Omega$

$$R_{22} = 39 (0.5858) \text{ k}\Omega = 22.85 \text{ k}\Omega$$

Therefore the nearest standard value of $22 \text{ k}\Omega$ was chosen for R_D .

The Butterworth Low-Pass Active Filter: This circuit was designed using the equal component approach for the frequency determinant capacitors and resistors in the circuit for critical frequency of 50Hz and a roll off of 40db per decade. A suitable standard value of 390nF was chosen for capacitance C_F so that R_F is:

$$R_F = \frac{1}{2\pi f_0 C}$$

$$R_F = \frac{1}{2\pi(50)(0.39 \times 10^{-9})} = 8.16 \text{ k}\Omega$$

The nearest standard value of resistor of $7.5 \text{ k}\Omega$ was chosen since there was no $8.16 \text{ k}\Omega$ in the standard value.

Expected voltage gain for a 2 pole equal component active filter is 1.5858 from standard voltage gain chart.

$$A_v = \frac{R_{22}}{R_1} = 1.5858 - 1 = 0.5858$$

The 6-pole Butterworth low-pass was designed by calculating the frequency and resistance values the same way as that of the 2-pole Butterworth low-pass since it is at the same critical frequency of 50Hz so it will carry the same value of C_F and R_F . However the voltage gain was calculated for each pole. These voltage gains are $A_{v1} = 1.0684$, $A_{v2} = 1.5858$, and $A_{v3} = 2.4824$. Therefore, $A_v \text{ total} = 4.2058$.

The individual voltage gains were used to get the values of R_{22} , R_{26} and R_{29} respectively by choosing the closest standard values in each case, in a pattern similar to the 2-pole Butterworth low-pass filter design.

All designed stages were put together to get the full circuit as shown in Figure 7.

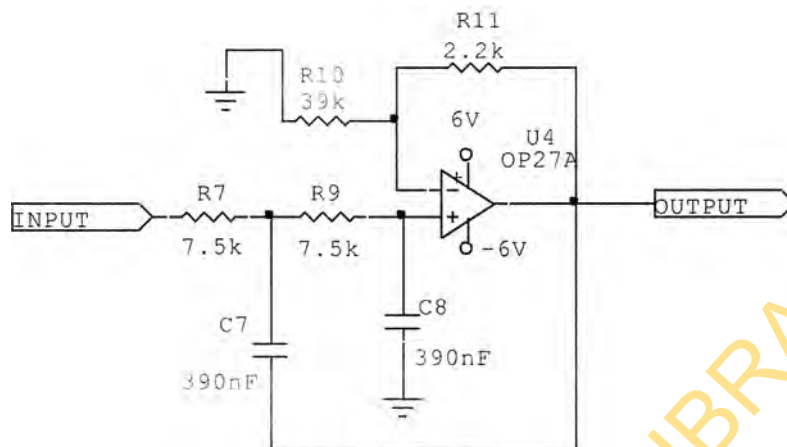


Figure 5: 2-Pole Butterworth Low-Pass Filter.

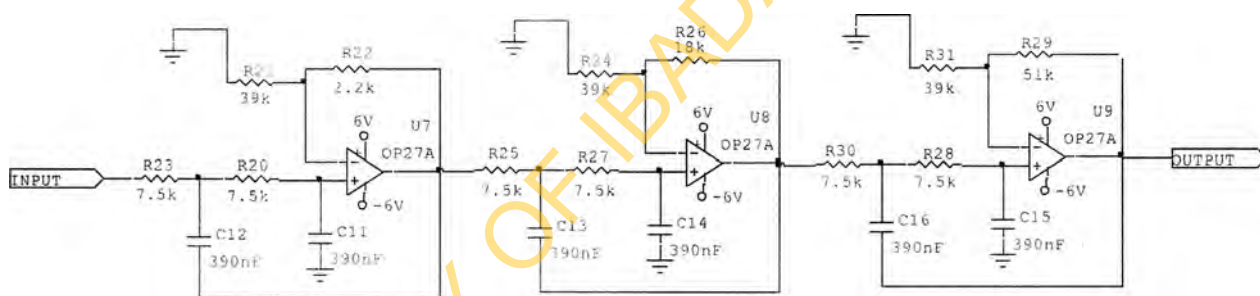


Figure 6: 6-Pole Butterworth Low-Pass Filter.

Electronic System Simulation: The simulation of the designed system was carried out using the circuit maker software (2000 version) before the construction. This was carried out to help analyze the possible characteristics of the system at each stage. This software has features like signal generators (oscillators), oscilloscopes, digital multimeters, signal sources and several types of components that can be used in circuit design. Figure 7 shows the layout of circuit-marker.

The required components in the software were connected to form the circuit as designed, then the simulated circuit was tested for the frequency response and signal transfer from one stage of

the circuit to another. This was achieved by driving the signals from the signal generators into the input of the simulated electronic circuit. The output was then analyzed using the oscilloscope, bode plot and voltmeter in the software.

The Calibration System: The output of the induction coil magnetometer designed in this work is a low frequency voltage. Therefore, there is a need for the calibration of the sensor to determine the conversion factor of the output r.m.s., voltage with the external magnetic field (Hs).

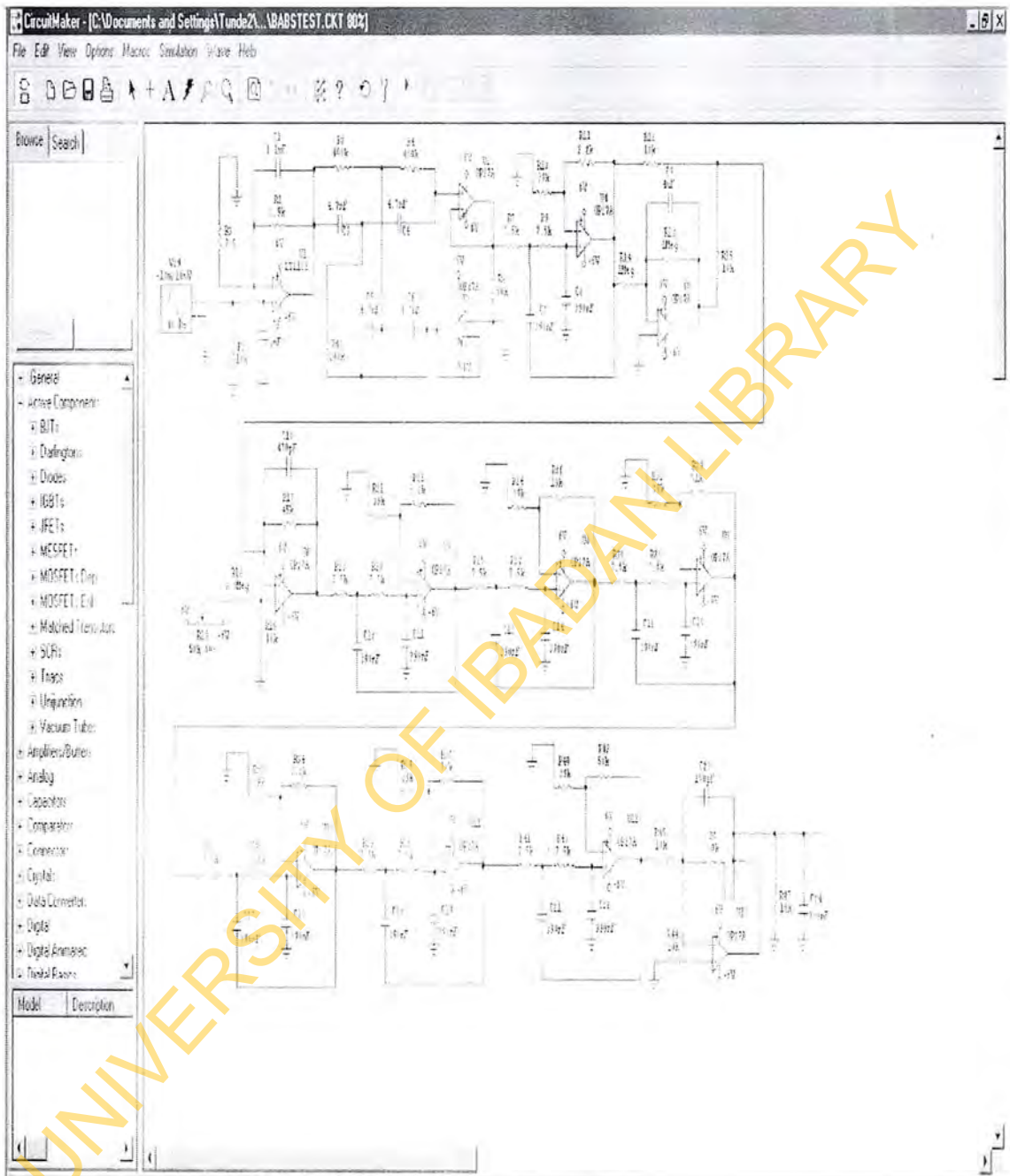


Figure 7: The Layout of Circuit-Maker.

A simple Calibration system using the Helmholtz coil pair was designed for this procedure, since the Helmholtz coil can generate very uniform magnetic field up to 25% or more of the covered area from the centre axis. The Helmholtz coil was

powered by a reliable current source with its input being varied using a Variac.

The GEM magnetometer was used to study and calibrate the output of the Helmholtz coil, with

different voltage inputs of the variac. The Helmholtz coil generated magnetic field measured in microtesla (μT). The calibration was within 0 – 30 μT range by adjusting input current supply with the variance.

The calibrated Helmholtz coil pair was then used for the calibration of the constructed induction coil magnetometer with the known microtesla (μT) outputs of the Helmholtz coil giving different ranges of output r.m.s voltage on the induction coil magnetometer constructed. The result of the calibration is shown in Figure 11.

The output of the induction coil sensor was plotted against the known magnetic fields applied on the constructed system from the Helmholtz coil.

TEST AND RESULTS

The simulated circuit was tested to examine the frequency response before the construction. The

constructed system was also tested using the signal generator (oscillator) to generate signals at the desired voltage ranges and frequencies. The output signals were obtained on the oscilloscope.

Simulated Frequency Response Results

Tests were carried out using the circuit maker software. The signal of 10mV was fed into the circuit in the software at different frequencies between 0 – 40Hz. The frequency response curve of the output voltage versus frequency shows the expected behavior for the type of circuit. There was a cut off at approximately 0.1 to 40Hz or shortly before 40Hz (36 Hz precisely). This cut off shows that the circuit to be designed perfectly attenuates unwanted frequencies as expected and passing other frequencies within the desired range. Figure 8 shows the voltage response curve which describes the expected behavior of the circuit.

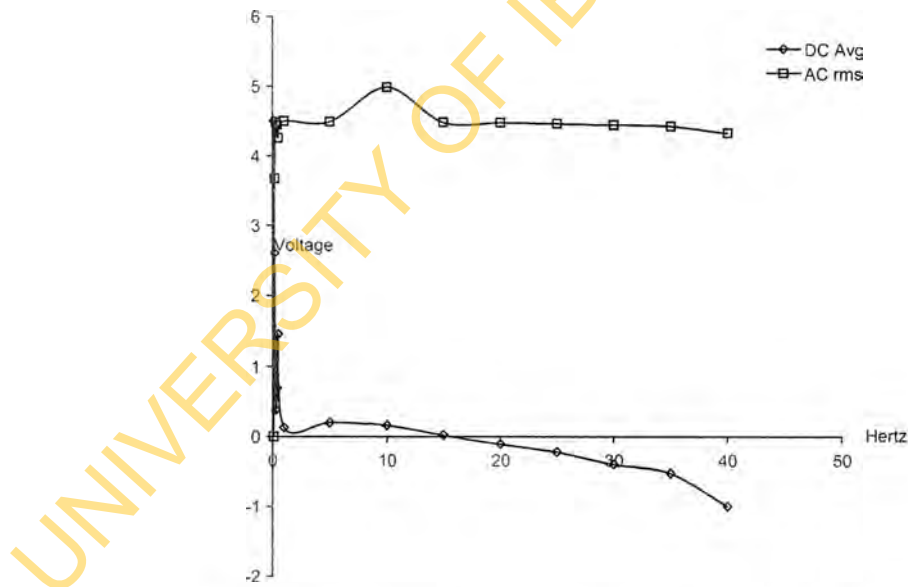


Figure 8: Simulated Frequency Response Curve for 10mV signal.

Actual Frequency Response Test for the Constructed Magnetometer

The constructed system was tested rigorously using the signal generator. The output generated was tested on the oscilloscope.

The signals generated from the oscillators were fed into the system and the DC averages were measured with the digital voltmeter for each signal. The AC r.m.s values of the output voltage were measured on the oscilloscope.

Firstly, a signal of 10mV was generated from the signal generator and fed into the constructed system at different frequencies within the range of 0 - 40Hz. The DC averages and the AC r.m.s values were plotted against the frequencies. This shows the expected frequency response with cut off at approximately 0.1 and at the higher frequencies above 40Hz. This was repeated for 0.1volt and 1volt signals from the signal generator

and similar frequency responses were observed from the frequency response curves.

The frequency response curves are shown in figures 8, 9, and 10, respectively.

Calibration Result

The result of the calibration is shown in Figure 11. The diagram shows that the output of the induction coil magnetometer is linear within the range of 0 – 30 μ T. The minimum strength of the magnetic field (Hs) which can be detected by the sensor is within 300 μ T - 400 μ T. This limit was determined by the smallest stable r.m.s. voltage measured by the magnetometer. The output r.m.s voltage is linear to the magnetic field strength with the regression coefficient of 0.9757. The sensitivity of the sensor, which was determined from the gradient of the graph, is 299mV/ μ T.

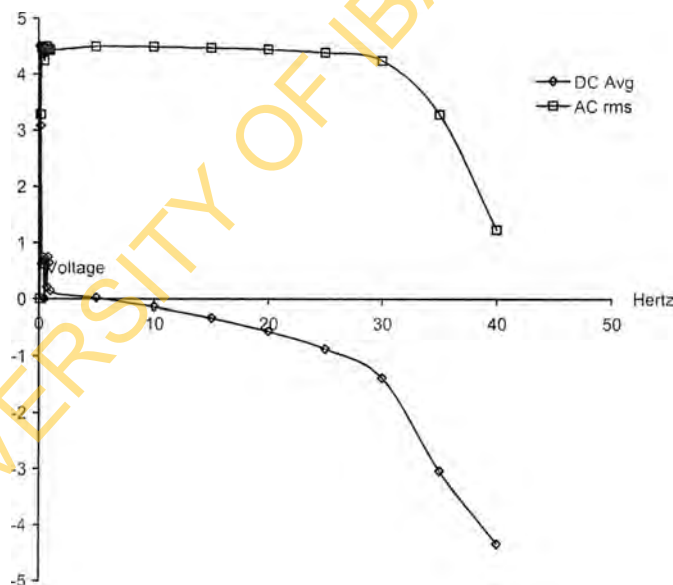


Figure 9: Frequency Response Curve for 0.1 Volt Signal.

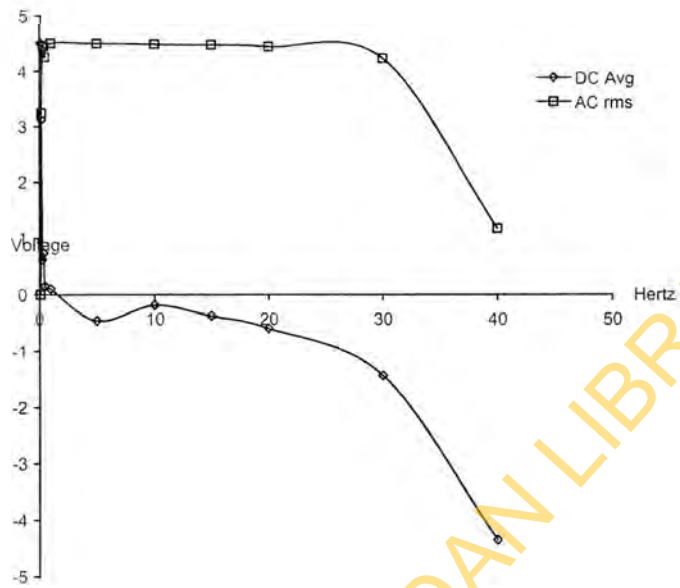


Figure 10: Frequency Response Curve for 1 Volt Signal.

Graph of output Voltage vs applied magnetic field, H_z (0 - 30 μ t)

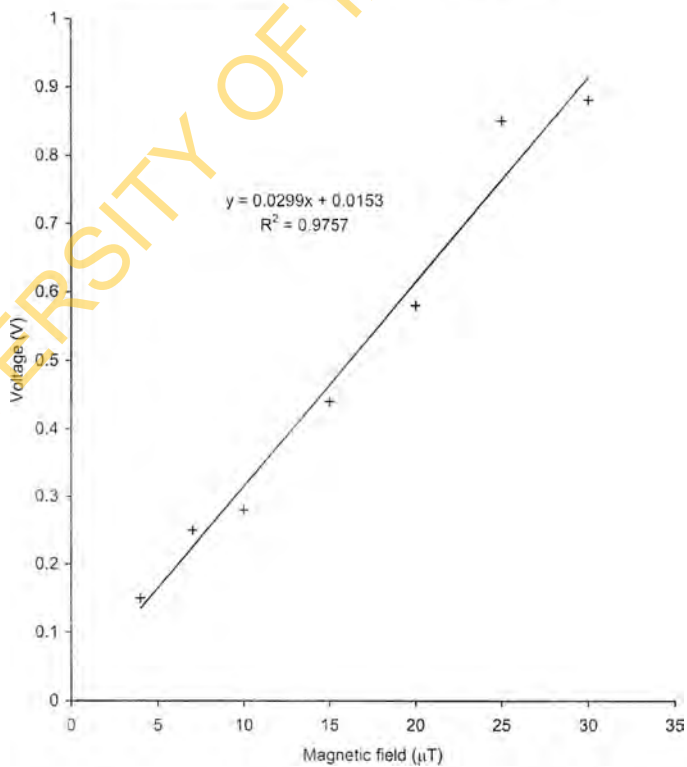


Figure 11: Graph of Output RMS Voltage versus Magnetic Field Strength.

CONCLUSION

The induction coil which served as the sensor and the electronic system for the induction coil magnetometer were designed and constructed. The design of the coil was done by winding of insulated wire around a combination of ferromagnetic alloy and air core at 4,500 turns to generate the electromotive force.

The design and construction of the electronic system which are the main part of this work comprise different stages of amplification and filtering processes.

The frequency response of the designed and constructed Magnetometer was identical with that of the simulated Magnetometer circuit. This constructed Magnetometer circuit amplifies with a reasonable voltage gain. It efficiently amplifies a very weak signal at the desired frequency range of 0.1Hz to 40Hz as expected.

REFERENCES

1. Dehmel, G. 1989. "Magnetic Field Sensors: Induction Coil (search coil) Sensors". Chapter 6. In *Sensors – A Comprehensive Survey*, Vol. 5. VCH Publishers: Birmingham, UK. 205-254.
2. Stuart, W.F. 1972. "Earth's Field Magnetometry". *Rep. Prog. Phys.* 35:803-881.
3. Campbell, W.H. 1969. "Induction Loop Antennas for Geomagnetic Field Variation Measurements". *ESSA Technical Report*. ERL123-ESL6.
4. Yamaguchi, M., S. Yabukami, and K.I. Arai. 2000. "Development of Multiplayer Planar Flux Sensing Coil and its Application to 1 MHz – 3.5 GHz Thin Film Permeance Meter". *Sensors and Actuators*. 81:212-215.
5. Ueda, H. and T. Watanabe. 1975. "Several Problems about Sensitivity and Frequency Response of an Induction Magnetometer". *Sci. Rep. Tohoku Univ. Ser. 5. Geophysics*. 22:107-127.

SUGGESTED CITATION

Adetoyinbo, A.A., O.S. Hammed, and B.O. Ogunsua. 2010. "Fabrication of an Induction Coil Magnetometer for Geomagnetic Field Measurement". *Pacific Journal of Science and Technology*. 11(2):107-117.



Pacific Journal of Science and Technology